



# A green and efficient hydration of alkynes catalyzed by hierarchically porous poly(ionic liquid)s solid strong acids



Duan-Jian Tao<sup>a</sup>, Fujian Liu<sup>b,\*</sup>, Lin Wang<sup>c</sup>, Lilong Jiang<sup>b</sup>

<sup>a</sup> College of Chemistry and Chemical Engineering, Institute of Advanced Materials, Jiangxi Normal University, Nanchang, PR China

<sup>b</sup> National Engineering Research Center of Chemical Fertilizer Catalyst (NERC-CFC), School of Chemical Engineering, Fuzhou University, Gongye Road No. 523, Fuzhou 350002, Fujian, PR China

<sup>c</sup> Wuhan Institute of Physics and Mathematics, Chinese Academy of Sciences, Wuhan 430071, PR China

## ARTICLE INFO

### Keywords:

Porous polymeric ionic liquids  
Alkynes hydration  
Hydroamination  
Solid acids  
Green and sustainable chemistry

## ABSTRACT

The catalytic conversion of alkynes into ketones *via* hydration has received considerable attention, because the ketones are very important intermediates in the chemical and pharmaceutical industries. The hydration of alkynes was usually performed with rather complicated processes in presence of liquid acids or highly toxic metal catalysts. We report here a novel metal free and efficient route to conversion of alkynes into ketones catalyzed by hierarchically porous poly(ionic liquid)s solid strong acids, which were synthesized from one-step, template-free copolymerization of divinylbenzene (DVB) with nitrogen containing monomers under solvothermal condition, further by post grafting with strong acid ionic liquid groups. The porous poly(ionic liquid)s solid acids have large BET surface areas, hierarchical nanopores and enhanced acid strength. A variety of alkynes could be effectively transformed into ketones catalyzed by the synthesized porous poly(ionic liquid)s solid acids under green and mild conditions, which were much better than those of Amberlyst 15, phosphotungstic acid and sulfuric acid. Furthermore, the porous poly(ionic liquid)s solid acids also show excellent activities and good reusability in direct hydroamination of amines with phenylacetylene. This work largely expands the wide applications of porous poly(ionic liquid)s solid strong acids in hydration and hydroamination, which develops a green, efficient and cost effective approach for conversion of low cost alkynes into high-value added ketones.

## 1. Introduction

Ketones are very important intermediates in the chemical and pharmaceutical industries, and they are popularly produced by the hydration of alkynes with 100% atomic economy [1,2]. However, the traditional alkynes hydration usually employs mercuric (II) salt, a highly toxic compound, as the catalyst in aqueous sulfuric acid, which strongly constrain their wide applications in the industry [3]. To overcome the toxicity of Hg salts, the usage of various organometallic catalysts such as compounds containing Au, Pt, Ag, Ru, and even biomimetic catalysts have been widely developed [4–13]. Despite enhanced conversions and selectivities were obtained, these catalysts also suffered from at least one of the following drawbacks: (1) expensive noble metals (Au, Pt, Ru, Ag, *etc*); (2) high reaction temperatures (> 100 °C); (3) large excess of water and additional acidic additives; (4) limited functional group compatibility. Recently, several Brønsted acids (e.g. TfOH, HNTf<sub>2</sub>) were found to exhibit very good catalytic activity for the hydration of alkynes [14,15]. However, the processes usually

require stoichiometric or excess amounts of acids, which lead to the difficulties in separating and recycling of acid catalysts. Therefore, it is still highly desirable to develop new kind of acid catalysts with high effectiveness for alkynes hydration under green and mild conditions.

Acidic ionic liquids (ILs), regarded as a new type of green reaction medium, have been successfully introduced into the area of acid catalysis owing to their unique properties such as negligible vapor pressure, remarkable solubility, and structural variety [16–19]. To promote separation and reusability of the homogeneous ILs catalysts, the synthesis of mesoporous polymeric ILs catalysts containing both the acidic sites and the IL groups has received considerable attention in these years [20,21]. Porous polymeric ILs, as highly active acid catalysts, should have several characteristics including large BET surface areas, strong acid strength, and enhanced exposure degree of active sites. However, many polymeric ILs reported in the previous literatures, have very low concentrations of acidic sites and rather poor porosities, which constrain them used as efficient solid acids in various acid-catalyzed reactions, especially in hydration reaction [22–25]. Therefore, it remains

\* Corresponding author.

E-mail address: [fjliu@usx.edu.cn](mailto:fjliu@usx.edu.cn) (F. Liu).

<https://doi.org/10.1016/j.apcata.2018.07.018>

Received 30 May 2018; Received in revised form 7 July 2018; Accepted 14 July 2018

Available online 17 July 2018

0926-860X/ © 2018 Elsevier B.V. All rights reserved.

a challenge to prepare porous polymeric ILs with large BET surface areas, enhanced acid strength, controllable and high contents of acid sites.

Recently, we reported the preparation of strongly acidic ILs functionalized, porous polymers with unique characteristics such as controllable hydrophilic–hydrophobic networks, hierarchical porosity, large BET surface areas and strong acid strength, which exhibit even higher activities than their homogeneous counterparts in biodiesel production [20]. In this work, we report here the synthesis of sponge-like nanoporous polymers functionalized with both the sulfonic group and the ionic liquids group (e.g., PDVB-[C<sub>3</sub>VP][SO<sub>3</sub>CF<sub>3</sub>], PDVB: polydivinylbenzene, VP: 4-vinyl pyridine, C<sub>3</sub>: 1,3-propanesultone, SO<sub>3</sub>CF<sub>3</sub>: HSO<sub>3</sub>CF<sub>3</sub> anion-exchanger), which were synthesized from solvothermal copolymerization of divinylbenzene (DVB) with functional monomers of 1-vinylimidazolate (vim) or 4-vinyl pyridine (VP) at 100 °C, followed by formation of quaternary ammonium salts using 1,3-propanesultone, and finally ion-exchanged with HSO<sub>3</sub>CF<sub>3</sub>, similar to the method we previously reported. The combination of structural characteristics such as large BET surface areas, hierarchical nanopores and much enhanced acid strength, the synthesized nanoporous polymer ionic liquid solid acids show extraordinary catalytic activities and improved reusability in both hydration of alkynes into ketones and hydroamination of amines with phenylacetylene, which were better than those of Amberlyst 15, phosphotungstic acid and sulfuric acid. This work largely expands the wide applications of porous poly(ionic liquid)s solid strong acids in hydration and hydroamination, which develops a green, efficient and cost-effective approach for the conversion of raw feedstocks into high value-added chemicals in the industry.

## 2. Experimental details

### 2.1. Chemicals and reagents

All reagents were of analytical grade and used as purchased without further purification. Divinylbenzene (DVB), 1-vinylimidazole, 4-vinyl pyridine Amberlyst 15 were purchased from Sigma-Aldrich Co. Azobisisobutyronitrile (AIBN), ethyl acetate, 1,3-propanesultone, HSO<sub>3</sub>CF<sub>3</sub>, H<sub>2</sub>SO<sub>4</sub>, HCl, trifluoroethanol, toluene, phosphotungstic acid and CH<sub>2</sub>Cl<sub>2</sub> were obtained from Beijing Chemical Agents Company.

### 2.2. Samples preparation

Nanoporous polymers could be synthesized from crosslinking of 1-vinylimidazolate (vim) or 4-vinylpyridine (VP) with DVB under solvothermal condition at 100 °C, where ethyl acetate was employed as the solvent. After quaternary ammonization and anion-exchange treatment, ILs functionalized nanoporous polymers were obtained [21].

In a typical synthesis of PDVB-VP-0.5 support, 2.0 g of DVB and 0.5 g of VP were introduced into a solution containing 0.07 g of AIBN and 30 mL of ethyl acetate. After stirring at room temperature for 3 h, the mixture was solvothermally treated at 100 °C for 24 h, followed by slow evaporation of the solvent at room temperature for 2 days. The product of PDVB-VP-0.5 with monolithic morphology was obtained. Correspondingly, PDVB-VP-0.2 could be synthesized with similar procedures, where 0.2 g of VP functional monomer was introduced into the mixture. Meanwhile, PDVB-vim-0.2 support could also be synthesized with similar procedure as that of PDVB-VP-0.2, where 0.2 g of vim functional monomer was introduced into the mixture.

PDVB-[C<sub>3</sub>VP][SO<sub>3</sub>CF<sub>3</sub>]-0.5 (C<sub>3</sub> stands for quaternary ammoniation reagent of 1,3-propanesultone) were synthesized by quaternary ammoniation of pristine PDVB-VP-0.5 support with 1,3-propanesultone, followed by ion exchanging with HSO<sub>3</sub>CF<sub>3</sub>. Typically, 1.0 g of PDVB-VP-0.5 was added into 25 mL of toluene under vigorous stirring, followed by addition of 0.25 g of 1,3-propanesultone. After quaternary ammoniation at 100 °C for 24 h, the product was collected by filtration, washing with abundant ethanol and drying at 60 °C. The resultant

sample was then treated with HSO<sub>3</sub>CF<sub>3</sub> in toluene solvent for 24 h at room temperature, washed with abundant CH<sub>2</sub>Cl<sub>2</sub> and dried at 80 °C for 8 h under vacuum condition, to give the final solid acid of PDVB-[C<sub>3</sub>VP][SO<sub>3</sub>CF<sub>3</sub>]-0.5. Correspondingly, PDVB-[C<sub>3</sub>VP][SO<sub>4</sub>H]-0.5 could also synthesized with similar procedures, where the exchange acid was sulfuric acid. PDVB-[C<sub>3</sub>vim][SO<sub>3</sub>CF<sub>3</sub>]-0.2 was prepared in a similar way, and PDVB-SO<sub>3</sub>H was prepared as literature for comparison [26].

### 2.3. Characterizations

Nitrogen isotherms were measured using a Micromeritics ASAP 3020 M system. The samples were outgassed for 10 h at 150 °C before the measurements. The pore-size distribution was calculated by using Barrett-Joyner-Halenda (BJH) model. FT-IR spectra were collected by using a Bruker 66 V FT-IR spectrometer. SEM images were performed on JEOL 6335 F field emission scanning electron microscope (FESEM) attached with a Thermo Noran EDX detector. Transmission electron microscopy (TEM) images were performed on a JEM-2100 F electron microscope (JEOL, Japan) with an acceleration voltage of 200 kV. CHNS elemental analysis was performed on a Perkin-Elmer series II CHNS analyzer 2400. XPS spectra were performed on a Thermo ESCALAB 250 with Al K $\alpha$  radiation at  $y = 901$  for the X-ray sources, the binding energies were calibrated using the C1s peak at 284.9 eV. <sup>13</sup>C solid state NMR experiments were carried out on a Varian Infinityplus-300 spectrometer at resonance frequencies of 75.38 MHz. The experiments were recorded using a 4 mm double-resonance MAS probe at a spinning rate of 10 kHz. The pulse width ( $\pi/2$ ) for <sup>13</sup>C was measured to be 4.1  $\mu$ s. A contact time of 4 ms and a recycle delay of 3 s were used for the <sup>13</sup>C CP/MAS measurement.

The solid-state <sup>31</sup>P NMR spectra over nanoporous polymer based solid acids were performed as the following procedures: prior to the sorption of trimethylphosphine (TMP) and trimethylphosphine oxide (TMPO) probe molecules, the samples were placed in glass tubes, which were connected to a vacuum line for dehydration. The samples were kept at a final temperature at 453 K for 24 h, with the pressure below 10<sup>-3</sup> Pa. Then, they were cooled. The preparation of TMPO adsorbed samples was performed according to the method proposed by Zheng et al. [27]. Prior to the NMR experiments, the sealed sample tubes were opened and the samples were transferred into NMR rotors with a Kel-F end cap under a dry nitrogen atmosphere in a glove box. <sup>31</sup>P NMR experiments were performed on a Bruker Ascend-500 spectrometer at a resonance frequency of 202.34 MHz for <sup>31</sup>P nucleus, with a 4 mm triple-resonance MAS probe at a spinning rate of 12 kHz. Pulse width ( $\pi/2$ ) for <sup>31</sup>P was measured to be 4.5  $\mu$ s. <sup>31</sup>P MAS NMR spectra with high power proton decoupling were recorded with a recycle delay of 30 s. The chemical shift of <sup>31</sup>P resonance was externally referenced to 1 M aqueous H<sub>3</sub>PO<sub>4</sub>.

### 2.4. Reaction procedures

A typical procedure for the ketone from alkynes hydration is as follows: Catalyst (44 mg) was added into the mixture of phenylacetylene (0.4 mmol) and deionized water (0.8 mmol) in trifluoroethanol (2.0 mL) in a 12 mL microwave tube. The resulting mixture was vigorously stirred at 1000 rpm at controlled temperature. After reaction for 18 h, the reaction mixture was centrifuged and the liquid was transferred to a bottle. Qualitative analyses of products were examined by a Thermo Trace 1300 GC-ISQ, and quantitative analyses were carried out by a GC-FID (Agilent 7890B). A capillary column HP-5 (methyl polysiloxane, 30 m  $\times$  0.32 mm  $\times$  1  $\mu$ m) was used to determine the composition of the samples with nitrogen as the carrier gas at a flow rate of 3 mL/min. The temperature of the column, the inlet and the detector was kept at 453, 473, and 523 K, respectively.

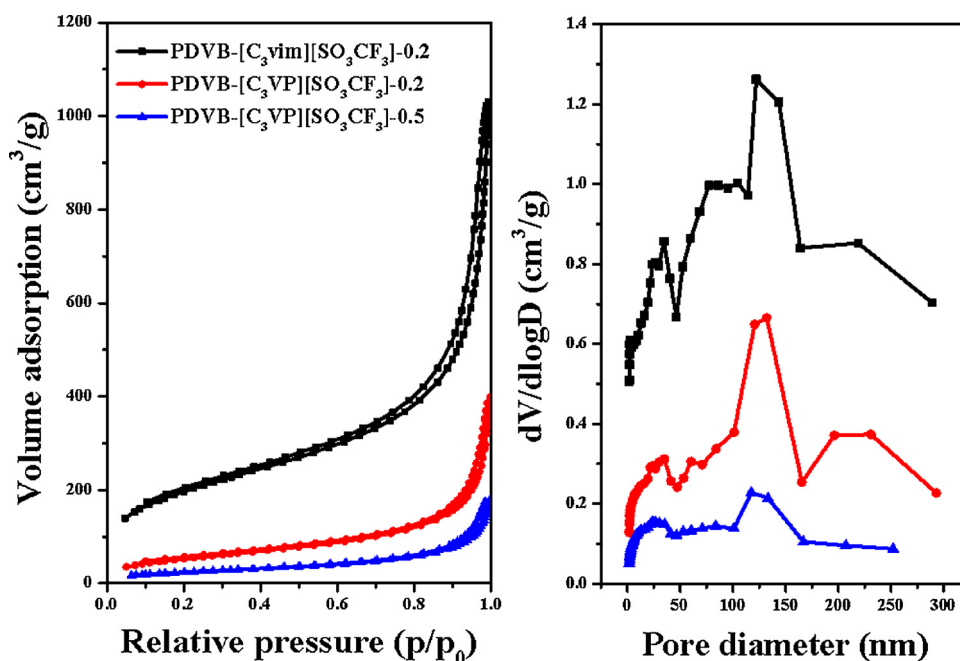


Fig. 1.  $N_2$  adsorption-desorption isotherms and pore size distribution obtained for PDVB-[C<sub>3</sub>vim][SO<sub>3</sub>CF<sub>3</sub>]-0.2, PDVB-[C<sub>3</sub>VP][SO<sub>3</sub>CF<sub>3</sub>]-0.2 and PDVB-[C<sub>3</sub>VP][SO<sub>3</sub>CF<sub>3</sub>]-0.5.

### 3. Results and discussion

#### 3.1. Structural characterizations

Fig. 1 shows  $N_2$  sorption-desorption isotherms at 77 K and pore size distribution of the synthesized PDVB-[C<sub>3</sub>vim][SO<sub>3</sub>CF<sub>3</sub>]-0.2, PDVB-[C<sub>3</sub>VP][SO<sub>3</sub>CF<sub>3</sub>]-0.2 and PDVB-[C<sub>3</sub>VP][SO<sub>3</sub>CF<sub>3</sub>]-0.5. Interestingly, all the samples show typical type-IV isotherms with relatively high volume adsorption, which increases steeply at the relative pressure of 0.85–1.0, indicating that abundant meso-macropores were formed in these samples. The pore size distribution cover a wide range from 0 to 300 nm, indicating hierarchical nanopores were formed in these samples. The calculated textural properties of the synthesized POPs are illustrated in Table 1, PDVB based poly(ionic liquid)s solid strong acids show large BET surface areas ranged from 92 to 698 m<sup>2</sup>/g, the corresponding pore volumes were ranged from 0.27 to 1.49 cm<sup>3</sup>/g. The pore size distributions curves of PDVB based poly(ionic liquid)s shows dual

Table 1  
The textural and acidic parameters of various acid catalysts.

Samples	Acid content (mmol/g) <sup>a</sup>	$S_{BET}$ <sup>b</sup> (m <sup>2</sup> /g)	$V_p$ <sup>c</sup> (cm <sup>3</sup> /g)	$D_p$ (nm) <sup>d</sup>
PDVB-[C <sub>3</sub> vim][SO <sub>3</sub> CF <sub>3</sub> ]-0.2	0.95	698	1.49	32.5&126.5
PDVB-[C <sub>3</sub> vim][SO <sub>3</sub> CF <sub>3</sub> ]-0.5	1.78	279	0.73	29.4&123.3
PDVB-[C <sub>3</sub> VP][SO <sub>3</sub> CF <sub>3</sub> ]-0.2	0.98	196	0.61	30.9&126.5
PDVB-[C <sub>3</sub> VP][SO <sub>3</sub> CF <sub>3</sub> ]-0.5	1.83	92	0.27	28.4&122.1
Amberlyst 15	4.7	45	0.31	40
H <sub>3</sub> O <sub>40</sub> PW <sub>12</sub> <sup>e</sup>	3.5	–	–	–
H <sub>2</sub> SO <sub>4</sub> <sup>e</sup>	20.4	–	–	–

<sup>a</sup> Measured by acid-base titration.

<sup>b</sup> Surface area calculated from the BET equation in the relative pressure range of 0.05–0.20.

<sup>c</sup> Single point total pore volume calculated at the relative pressure of 0.99.

<sup>d</sup> Pore size distribution estimated from BJH model.

<sup>e</sup> Calculated from molecular formula.

peaks centered at around 30 and 120 nm, which were distributed in the range of meso-macroporous scale. Combination of large BET surface areas and abundant meso-macropores in PDVB based poly(ionic liquid)s, which was favorable for the fast diffusion of various substrates, enhancement of accessibility of acidic sites in these samples. The acid contents of PDVB based poly(ionic liquid)s were ranged from 0.95 to 1.83 mmol/g (Table 1), which were lower than various traditional acid catalysts such as Amberlyst 15 (4.7 mmol/g), H<sub>3</sub>O<sub>40</sub>PW<sub>12</sub> (3.5 mmol/g), and H<sub>2</sub>SO<sub>4</sub> (20.4 mmol/g).

Fig. 2 shows SEM images of PDVB-[C<sub>3</sub>vim][SO<sub>3</sub>CF<sub>3</sub>]-0.2 and PDVB-[C<sub>3</sub>VP][SO<sub>3</sub>CF<sub>3</sub>]-0.2. Both samples showed monolith morphology with rather rough surface and sponge-like characteristics, and abundant macropores were found in these samples. The pore sizes were larger than 100 nm, which was in consistent with  $N_2$  adsorption results. On the other hand, TEM images of the synthesized samples were also systematically studied. TEM is a reliable technique for characterization the internal nanopores of porous materials. Fig. 3 shows the TEM images of PDVB-[C<sub>3</sub>vim][SO<sub>3</sub>CF<sub>3</sub>]-0.2, PDVB-[C<sub>3</sub>VP][SO<sub>3</sub>CF<sub>3</sub>]-0.2 and PDVB-[C<sub>3</sub>VP][SO<sub>3</sub>CF<sub>3</sub>]-0.5. Interestingly, all the samples showed the hierarchical meso-macropores characteristics, which are in consistent with  $N_2$  adsorption and SEM results. The mesopore sizes were distributed in the range from 20 to 40 nm, in good agreement with  $N_2$  adsorption results.

Fig. 4 shows <sup>13</sup>C solid state NMR spectrum of PDVB-[C<sub>3</sub>VP][SO<sub>3</sub>CF<sub>3</sub>]-0.2. Notably, the chemical shifts at around 41 and 46 ppm should be assigned to methylene bridges in PDVB-VP support and C<sub>3</sub> alkyl chain. The chemical shift at around 138 ppm should be assigned to the carbon atom connected with nitrogen in pyridinic ring. The chemical shifts at around 129, 145 and 150 ppm should be assigned to the carbon atoms in DVB and pyridinic ring without connecting with nitrogen. The <sup>13</sup>C NMR spectrum confirms the successful grafting of strong acid ionic liquids onto the network of PDVB-VP, which gives PDVB-[C<sub>3</sub>VP][SO<sub>3</sub>CF<sub>3</sub>]-0.2 solid acids.

To further confirm the acidity of the synthesized nanoporous poly(ionic liquid)s solid acids. Various characterization of FT-IR, XPS and <sup>31</sup>P solid state NMR spectra were investigated. Fig. 5 shows FT-IR spectra of PDVB-[C<sub>3</sub>vim][SO<sub>3</sub>CF<sub>3</sub>]-0.2, PDVB-[C<sub>3</sub>VP][SO<sub>3</sub>CF<sub>3</sub>]-0.2, PDVB-[C<sub>3</sub>VP][SO<sub>3</sub>CF<sub>3</sub>]-0.5 and five times recycled PDVB-[C<sub>3</sub>VP][SO<sub>3</sub>CF<sub>3</sub>]-0.5. Notably, the vibration at around 1036 and 1220 cm<sup>-1</sup>

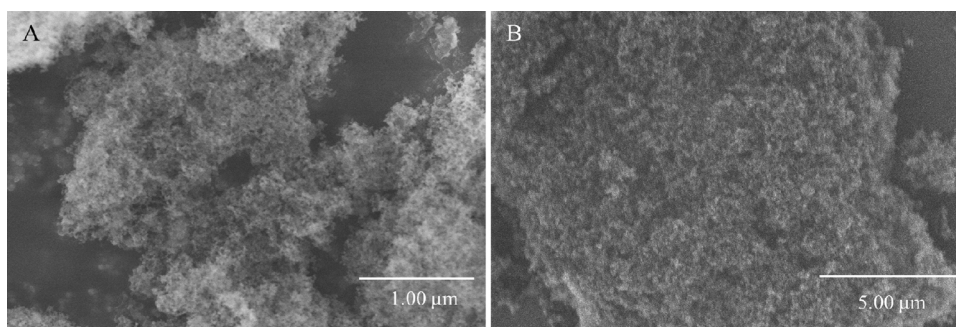


Fig. 2. SEM images of (a) PDVB-[C<sub>3</sub>vim][SO<sub>3</sub>CF<sub>3</sub>]-0.2 and (b) PDVB-[C<sub>3</sub>VP][SO<sub>3</sub>CF<sub>3</sub>]-0.2.

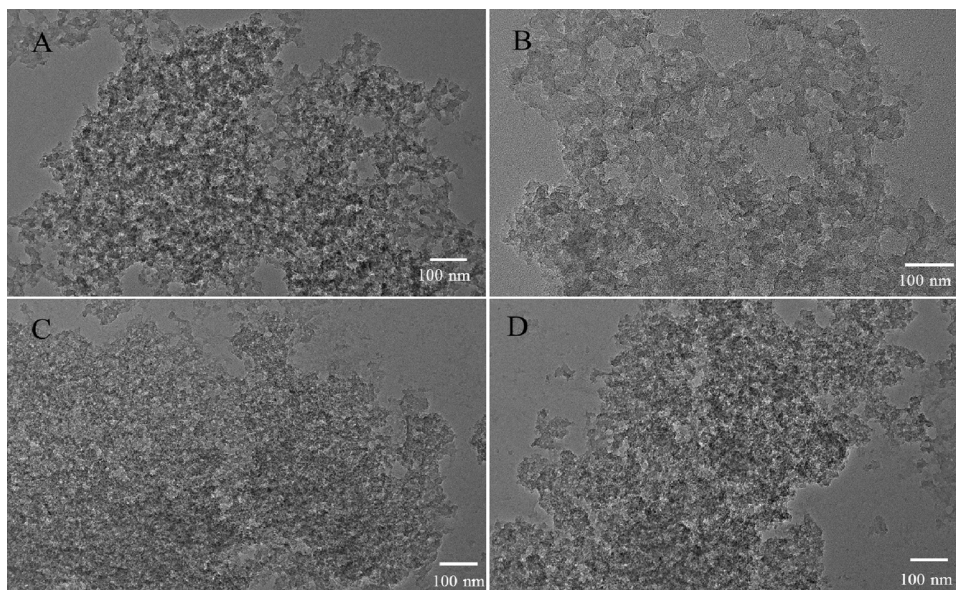


Fig. 3. TEM images of (A&B) PDVB-[C<sub>3</sub>vim][SO<sub>3</sub>CF<sub>3</sub>]-0.2, (C) PDVB-[C<sub>3</sub>VP][SO<sub>3</sub>CF<sub>3</sub>]-0.2 and (D) PDVB-[C<sub>3</sub>VP][SO<sub>3</sub>CF<sub>3</sub>]-0.5.

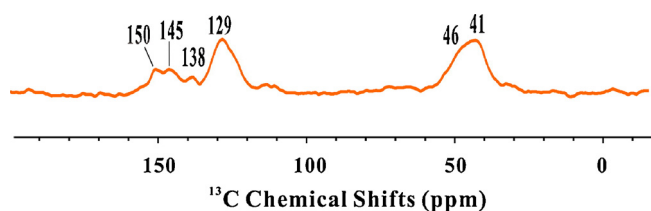


Fig. 4. <sup>13</sup>C solid state NMR spectrum of PDVB-[C<sub>3</sub>VP][SO<sub>3</sub>CF<sub>3</sub>]-0.2.

associated with the C–S and S=O vibrations could be observed in these samples. The vibration at around 1170 cm<sup>-1</sup> associated with the C–F and S–O vibration could also be observed in these samples, indicating the successful introduction of acid ionic liquid and sulfonate groups in these samples [20,26,28,29].

Fig. 6 shows X-ray photoelectron spectroscopy (XPS) of PDVB-[C<sub>3</sub>VP][SO<sub>3</sub>CF<sub>3</sub>]-0.5 and PDVB-[C<sub>3</sub>vim][SO<sub>3</sub>CF<sub>3</sub>]-0.5. The samples show the signals of C1s, N1s, O1s, S2p and F1s. The signal of S2p associated with sulfonate group was centered at around 168.5 eV. The C1s peaks at around 284.6, 286.2, and 291.9 eV are assigned to C–C, C–N, and C–F bond [20]. The N1s peaks are centered at around 401.9 eV, which indicates the successful quaternary ammonization of N atom in VP and vim building units with 1,3-propanesultone [20]. The O1s peaks at around 533.0 and 535.0 eV are assigned to the oxygen atoms in the -SO<sub>3</sub>H and -SO<sub>2</sub>CF<sub>3</sub>, respectively [20]. The F1s peaks at around 535.0 eV are assigned to -SO<sub>2</sub>CF<sub>3</sub> group [20]. The above results further confirm the successful grafting of acidic ionic liquid and

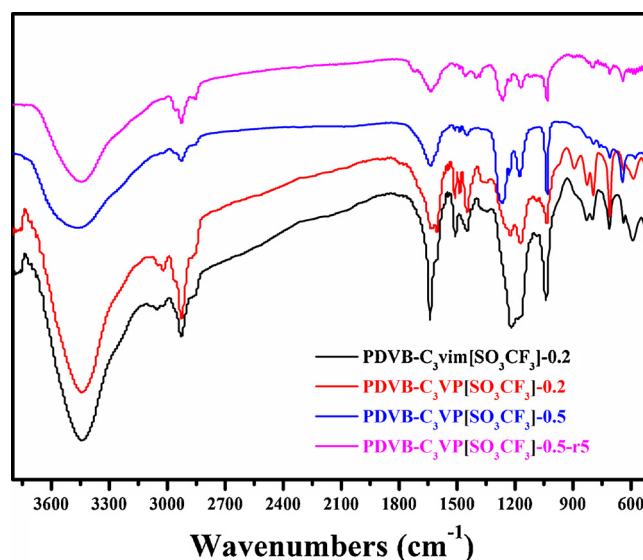


Fig. 5. FT-IR spectra of PDVB-[C<sub>3</sub>vim][SO<sub>3</sub>CF<sub>3</sub>]-0.2, PDVB-[C<sub>3</sub>VP][SO<sub>3</sub>CF<sub>3</sub>]-0.2, PDVB-[C<sub>3</sub>VP][SO<sub>3</sub>CF<sub>3</sub>]-0.5 and five recycled PDVB-[C<sub>3</sub>VP][SO<sub>3</sub>CF<sub>3</sub>]-0.5.

sulfonate groups in the synthesized PDVB-VP and PDVB-vim.

To further study the acidity of the synthesized solid acids, <sup>31</sup>P MAS NMR spectra of trimethylphosphine (TMP) and trimethylphosphine oxide (TMPO) adsorbed on the synthesized samples was investigated. It

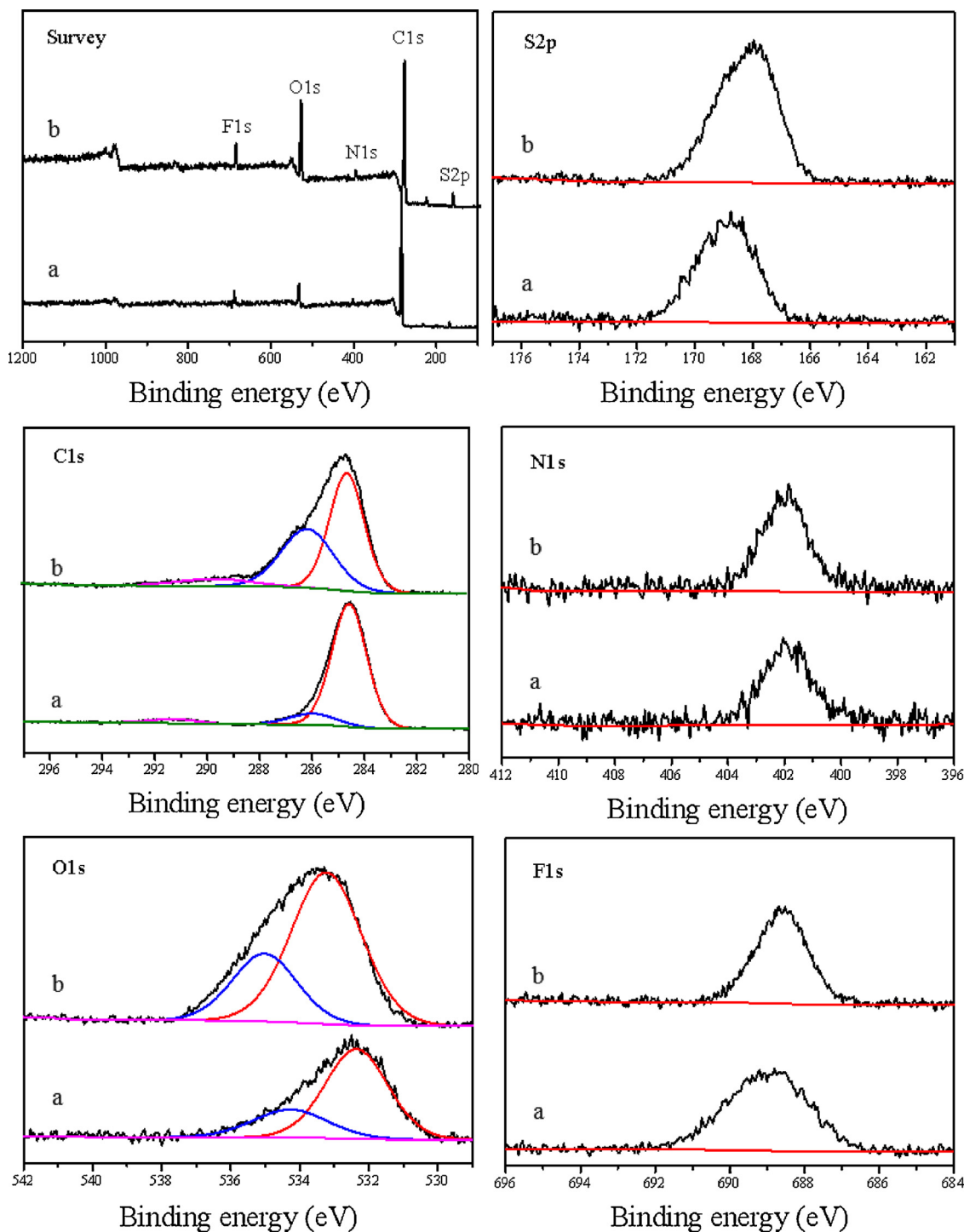


Fig. 6. X-ray photoelectron spectroscopy of (a) PDVB-[C<sub>3</sub>vim][SO<sub>3</sub>CF<sub>3</sub>]-0.5 and (b) PDVB-[C<sub>3</sub>VP][SO<sub>3</sub>CF<sub>3</sub>]-0.5.

is well known that <sup>31</sup>P MAS solid state NMR spectra is a *state of the art* technique for acidity characterization of various acid catalysts, and such approach has been extensively used to determine the acidic properties (i.g., acidic type, acidic strength and acidic amount) of various solid acids, including zeolites, sulfated mesoporous metal oxides and heteropolyacids [27,30–35]. Fig. 7a shows room temperature <sup>31</sup>P MAS NMR spectra of TMP adsorbed on PDVB-[C<sub>3</sub>VP][SO<sub>3</sub>CF<sub>3</sub>]-0.5. <sup>31</sup>P NMR of adsorbed TMP has been demonstrated to be a sensitive and reliable technique for the determination of the Brønsted and Lewis acid sites in the solid acids. The adsorption of TMP on the Brønsted acid will give rise to <sup>31</sup>P resonances in a rather narrow range (ca. –2 ~

–5 ppm), and TMP bound to Lewis acid sites, may result in <sup>31</sup>P peaks in the range of ca. –20 ~ –60 ppm [29,30]. As shown in Fig. 7a, using TMP as a probe molecule, the <sup>31</sup>P resonance at –3.3 ppm was assigned to the protonated adducts, [(CH<sub>3</sub>)<sub>3</sub>P-H]<sup>+</sup>, attributed by the reaction of TMP and the Brønsted acidic protons. The <sup>31</sup>P resonance at –62 ppm was assigned to the physical adsorbed TMP in the sample [34]. The <sup>31</sup>P resonance at 26.8 ppm should be attributed to the signal of mobile TMP in the sample [34].

In order to reveal the acid strength of the synthesized PDVB-[C<sub>3</sub>VP][SO<sub>3</sub>CF<sub>3</sub>]-0.5, TMPO as the probe molecular adsorbed on the surface of PDVB-[C<sub>3</sub>VP][SO<sub>3</sub>CF<sub>3</sub>]-0.5 was also investigated. The corresponding

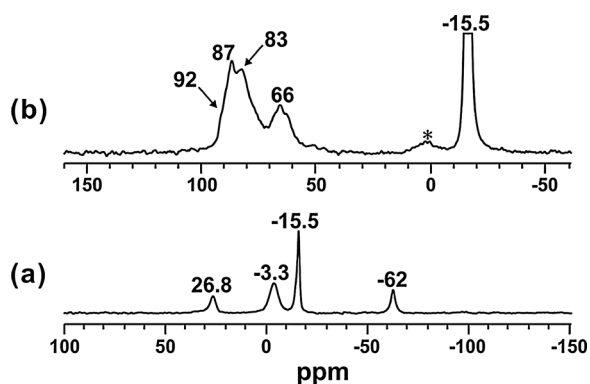


Fig. 7. Room temperature  $^{31}\text{P}$  MAS NMR spectra of (a) TMP and (b) TMPO adsorbed on PDVB-[C<sub>3</sub>VP][SO<sub>3</sub>CF<sub>3</sub>]-0.5.

**Table 2**  
Hydration reaction of phenylacetylene over different catalysts.<sup>a</sup>

Entry	Catalysts	Conversion (%)	Yield (%)
1	PDVB-[C <sub>3</sub> VP][SO <sub>3</sub> CF <sub>3</sub> ]-0.5	99	98
2	PDVB-[C <sub>3</sub> VP][SO <sub>4</sub> H]-0.5	90	81
3	PDVB-[C <sub>3</sub> VP][SO <sub>3</sub> CF <sub>3</sub> ]-0.2	95	89
4	PDVB-[C <sub>3</sub> vim][SO <sub>3</sub> CF <sub>3</sub> ]-0.5	96	90
5	PDVB-[C <sub>3</sub> vim][SO <sub>4</sub> H]-0.5	53	45
6	PDVB-[C <sub>3</sub> vim][SO <sub>3</sub> CF <sub>3</sub> ]-0.2	67	63
7	PDVB-SO <sub>3</sub> H	39	35
8	Amberlyst 15	18	8
9	H <sub>3</sub> O <sub>4</sub> PW <sub>12</sub>	78	56
10 <sup>b</sup>	Sulfuric acid	62	36

<sup>a</sup> Reaction condition: Phenylacetylene (0.4 mmol), H<sub>2</sub>O (0.8 mmol), CF<sub>3</sub>CH<sub>2</sub>OH (2 mL), catalyst (10 wt.% of phenylacetylene), 40 °C, 18 h.

<sup>b</sup> Catalyst (0.0005 g).

**Table 3**  
Hydration reaction of phenylacetylene over different solvents.<sup>a</sup>

Entry	Solvent	Yield (%)
1	CF <sub>3</sub> CH <sub>2</sub> OH	97
2	H <sub>2</sub> O	< 1
3	CH <sub>3</sub> CH <sub>2</sub> OH	< 1
4	DMSO	< 1
5	CH <sub>3</sub> CN	< 1
6	toluene	< 1
7	–	< 1

<sup>a</sup> Reaction condition: Phenylacetylene (0.4 mmol), H<sub>2</sub>O (0.8 mmol), solvent (2 mL), PDVB-[C<sub>3</sub>VP][SO<sub>3</sub>CF<sub>3</sub>]-0.5 catalyst (10 wt.% of phenylacetylene), 40 °C, 18 h.

$^{31}\text{P}$  solid-state NMR spectrum was shown in Fig. 7b. Interestingly, multiple  $^{31}\text{P}$  resonances at around 66, 83, 87 ppm were observed in the PDVB-[C<sub>3</sub>VP][SO<sub>3</sub>CF<sub>3</sub>]-0.5, which are assigned to various acid sites with different strength present in the sample. The resonance peak at around 66 ppm may be assigned to carboxylic acid site, which was resulted from partially oxidation of polymer networks. The resonances at around 83 and 87 ppm should be assigned to the grafted sulfonate group and immobilized acid ionic liquid site, which exhibit strong acid strength in comparison with variously reported solid acids [34]. Notably, a  $^{31}\text{P}$  resonance at -15.5 ppm could be observed in both TMP and TMPO adsorbed samples, which may be attributed to the residual phosphorus in the sample. This signal was not derived from the interactions between TMP or TMPO and PDVB-[C<sub>3</sub>VP][SO<sub>3</sub>CF<sub>3</sub>]-0.5. The  $^{31}\text{P}$  NMR spectra certified the successful introduction of strong acid ionic liquid group in PDVB-[C<sub>3</sub>VP][SO<sub>3</sub>CF<sub>3</sub>]-0.5, in good with FT-IR and XPS results.

### 3.2. Catalytic performance of porous poly(ionic liquid)s solid strong acids

Firstly, the catalytic performance of nanoporous poly(ionic liquid)s solid strong acids for hydration reaction of phenylacetylene was screened. The results are summarized in Table 2. It was found that under mild condition of reaction temperature of 40 °C for 18 h, PDVB-[C<sub>3</sub>VP][SO<sub>3</sub>CF<sub>3</sub>]-0.5 had the highest catalytic activity in the hydration reaction of phenylacetylene with a 98% yield of acetophenone (entries 1–7). This could be directly assigned to the super acid strength and high acid content of the PDVB-[C<sub>3</sub>VP][SO<sub>3</sub>CF<sub>3</sub>]-0.5 catalyst. Although PDVB-[C<sub>3</sub>VP][SO<sub>3</sub>CF<sub>3</sub>]-0.2 has larger BET surface area than PDVB-[C<sub>3</sub>VP][SO<sub>3</sub>CF<sub>3</sub>]-0.5, the limited acid content of PDVB-[C<sub>3</sub>VP][SO<sub>3</sub>CF<sub>3</sub>]-0.2 results in its lower activity in comparison with of PDVB-[C<sub>3</sub>VP][SO<sub>3</sub>CF<sub>3</sub>]-0.5. Similar trend could also be found in the PDVB-[C<sub>3</sub>vim][SO<sub>3</sub>CF<sub>3</sub>] samples. Also, relatively large surface area is favorable for exposure of catalytically active sites to reactants, and the abundant mesoporosity has an advantage for mass transfer. Moreover, the hydration of phenylacetylene was also examined using traditional liquid acids (H<sub>2</sub>SO<sub>4</sub>, heteropolyacid) and solid acid (Amberlyst 15) as catalysts (entries 8–10). It can be seen that PDVB-[C<sub>3</sub>VP][SO<sub>3</sub>CF<sub>3</sub>]-0.5 show much higher catalytic activity than those conventional acid catalysts. It is reasoned that on the basis of the same amount of acidic sites, PDVB-[C<sub>3</sub>VP][SO<sub>3</sub>CF<sub>3</sub>]-0.5 show much enhanced acid strength in comparison with these liquid acids. Also, the heterogeneous catalyst Amberlyst 15 has a relatively large mass transfer resistance, thus resulting in a low yield of acetophenone. Therefore, the above results demonstrated that PDVB-[C<sub>3</sub>VP][SO<sub>3</sub>CF<sub>3</sub>]-0.5 is considered to be a promising superacid catalyst with high activity for hydration of phenylacetylene.

### 3.3. Optimization of reaction parameters

To optimize the reaction conditions for PDVB-[C<sub>3</sub>VP][SO<sub>3</sub>CF<sub>3</sub>]-0.5 in hydration of phenylacetylene to prepare acetophenone, the effects of solvent, reaction time, reaction temperature, and catalyst loading on the yield of acetophenone were investigated. It can be seen from Table 3 that the solvent has a significant effect on the hydration reaction. Compared with other solvents, trifluoroethanol (CF<sub>3</sub>CH<sub>2</sub>OH) would be much more favorable to the hydration reaction. Given that alkyne's hydration is generally via a vinyl carbocation intermediate [36], CF<sub>3</sub>CH<sub>2</sub>OH has the ability to stabilize a vinyl carbocation intermediate and thereby cause the hydration reaction to proceed more efficient than those of reactions occurring in other solvents [14]. Moreover, the effect of reaction temperature was investigated in the range of 30–60 °C. Fig. 8a shows that the hydration could be completely carried out at the optimal reaction temperature of 40 °C, and thus the yield of acetophenone was given to 98%. This suggests that the favorable temperature in this work is much milder than those in most of reported literatures. Then, Fig. 8b shows the effect of catalyst loading on the hydration reaction. With an increase in the relative amount of PDVB-[C<sub>3</sub>VP][SO<sub>3</sub>CF<sub>3</sub>]-0.5, the reaction rate was speeded up and thus a higher yield was obtained. For example, when the dosage of PDVB-[C<sub>3</sub>VP][SO<sub>3</sub>CF<sub>3</sub>]-0.5 increased from 4 to 10%, the yield significantly increased from 63 to 98%. However, the catalyst loading was further added to 12%, only a little increase in the yield was examined. This indicates that over a certain catalyst loading, too much catalyst amount is not imperative. Thus, in view of the cost of catalyst, 10 wt.% is taken as the optimum catalyst loading and used in bulk of hydration experiments. Further, the reaction time was examined in the range of 12–24 h as shown in Fig. 8c. The yield of acetophenone gradually increases to 98% in the first 18 h but keeps no obvious change at longer reaction times. Thus, 18 h is chosen as the optimal reaction time. The reusability and stability of catalyst are also the key influential factors for potentially industrial application. After the completion of a reaction, the system with catalyst PDVB-[C<sub>3</sub>VP][SO<sub>3</sub>CF<sub>3</sub>]-0.5 was centrifuged. Follow on removing the liquid part and washing silt substance with dichloromethane, dried it in vacuum oven at 50 °C for 6 h. After that, there

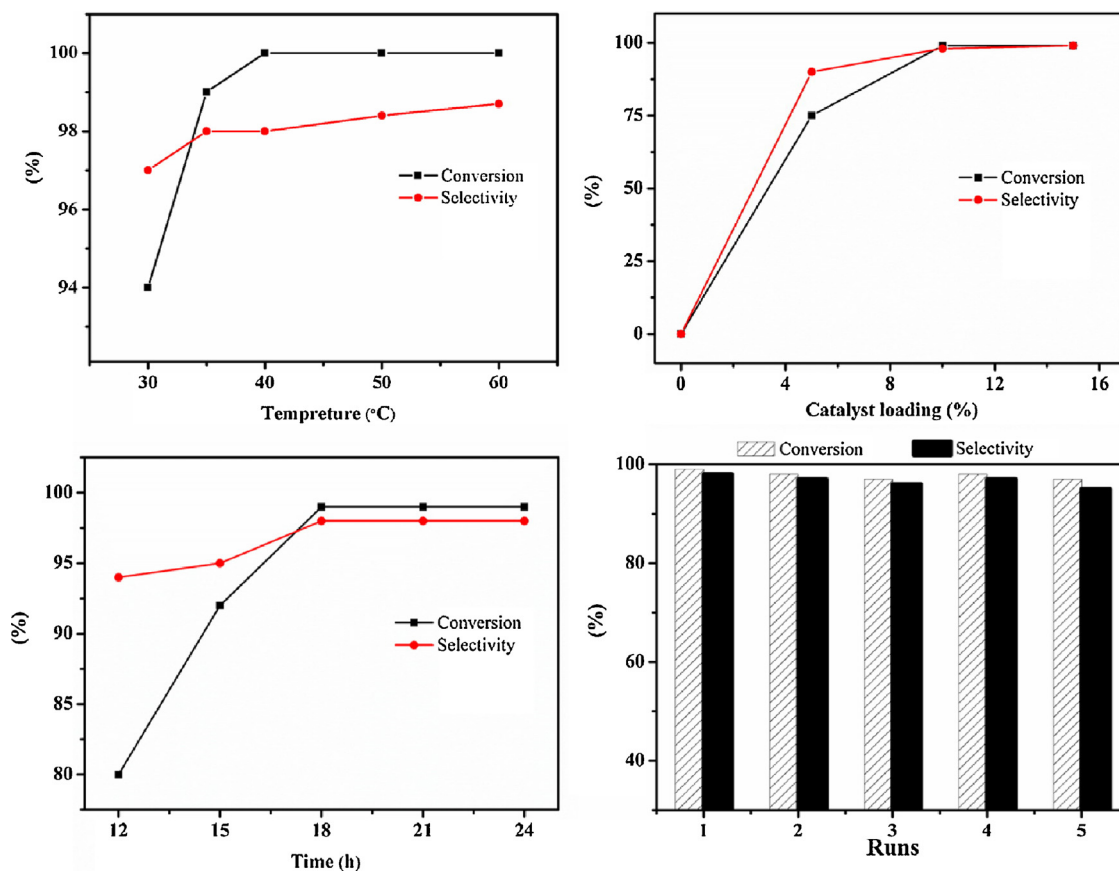


Fig. 8. Effect of (a) reaction temperature, (b) catalyst loading, (c) reaction time on hydration of phenylacetylene, and (d) recycling test of PDVB-[C<sub>3</sub>VP][SO<sub>3</sub>CF<sub>3</sub>]-0.5.

Table 4

Hydration of various alkynes catalyzed by PDVB-[C<sub>3</sub>VP][SO<sub>3</sub>CF<sub>3</sub>]-0.5<sup>a</sup>.

Entry	Alkyne	Product	Yield (%)
1			98
2			99
3 <sup>b</sup>			85
4 <sup>c</sup>			99
5 <sup>d</sup>			99
6 <sup>e</sup>			99

<sup>a</sup>Reaction condition: Alkyne (0.4 mmol), H<sub>2</sub>O (0.8 mmol), CF<sub>3</sub>CH<sub>2</sub>OH (2 mL), catalyst (10 wt.% of alkyne), 40 °C, 18 h. <sup>b,c</sup> 50 °C. <sup>d,e</sup> 90 °C, 24 h.

was a step called catalyst activation. The formed suspension, as the ratio of sample: dichloromethane: triflic acid = 1 g : 25 mL : 2 mL, was stirred at room temperature for 24 h. Next step, centrifuged, washed and dried, recycled PDVB-[C<sub>3</sub>VP][SO<sub>3</sub>CF<sub>3</sub>]-0.5 was used in hydration reaction. The above operation was repeated five times to test its activity as well as stability. As shown in Fig. 8d, no significant decrease in the yield of acetophenone was examined during the five successive recycles. Thus, the catalyst PDVB-[C<sub>3</sub>VP][SO<sub>3</sub>CF<sub>3</sub>]-0.5 was stable enough to be recycled for the hydration of phenylacetylene. PDVB-[C<sub>3</sub>VP][SO<sub>3</sub>CF<sub>3</sub>]-0.5 was considered to be steadily recycled for the hydration reaction.

### 3.4. Applicability of PDVB-[C<sub>3</sub>VP][SO<sub>3</sub>CF<sub>3</sub>]-0.5 catalyst

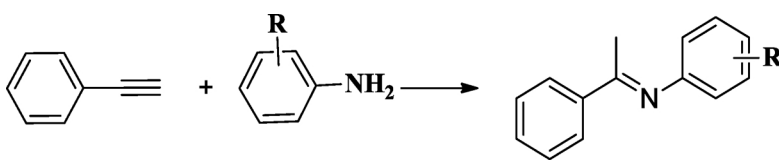
The applicability of PDVB-[C<sub>3</sub>VP][SO<sub>3</sub>CF<sub>3</sub>]-0.5 catalyst was examined for catalyzing hydration of different alkyne substrates. The results were presented in Table 4. With the substituent electron withdrawing group -Br and electron donating groups -CH<sub>3</sub>, -OCH<sub>3</sub> attached to the aromatic ring, the desired ketones could be obtained with excellent yields (85–99 %) under mild conditions (entries 1–4). Besides aromatic alkynes, the scope of this catalytic system was also explored for the hydration of aliphatic alkynes. It was indicated that the hydration of 1-octyne and 1,2-diphenylacetylene required a relatively long time and high temperature, resulting in corresponding the target products with 99% yield (entries 5, 6).

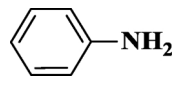
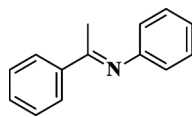
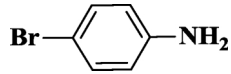
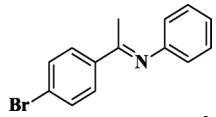
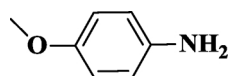
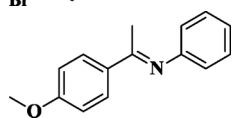
In addition, we tried to inspect the adaptation of PDVB-[C<sub>3</sub>VP][SO<sub>3</sub>CF<sub>3</sub>]-0.5 in a consecutive reaction, hydroamination of phenylacetylene with different amines (Table 5). The catalyst PDVB-[C<sub>3</sub>VP][SO<sub>3</sub>CF<sub>3</sub>]-0.5 showed the high activity with a 81% yield of imine. Notably, the hydroamination of aromatic amines with electron-donating or withdrawing group was further performed with almost 100% yields, although the reaction time prolongs to 50 h. These results demonstrate that poly(ionic liquid)s solid strong acid catalyst PDVB-[C<sub>3</sub>VP][SO<sub>3</sub>CF<sub>3</sub>]-0.5 exhibits the broad functional group compatibility in the hydration and hydroamination reactions, showing the potential industrial synthesis of high-value added ketones and imines.

## 4. Conclusions

In summary, hierarchically nanoporous poly(ionic liquid)s solid strong acids were prepared from copolymerization of DVB with nitrogen containing monomers under solvothermal condition without using additional templates, further by post grafting with strong acid ionic liquid groups. The synthesized porous ionic polymer based solid

**Table 5**  
Hydroamination of phenylacetylene with various amines <sup>a</sup>.



Entry	Amine	Product	Yield (%)
1			81
2			100
3			100

<sup>a</sup> Reaction condition: Phenylacetylene (0.4 mmol), H<sub>2</sub>O (0.8 mmol), amine (0.4 mmol), CF<sub>3</sub>CH<sub>2</sub>OH (2 mL), catalyst (0.048 g), 110 °C, 50 h.

acids show excellent activities and good reusability in direct hydration of alkynes into ketones without using any co-catalysts, much better than commercial acids such as Amberlyst 15, phosphotungstic acid and sulfuric acid. In addition, the synthesized poly(ionic liquid)s solid acids also show enhanced activities in hydroamination of alkynes with amines. This work develops efficient porous polymers ionic liquid solid strong acids in hydration and hydroamination of alkynes, which offers a green and metal free approach for transformation of low cost alkynes into high-value added ketones in the industry.

### Acknowledgements

This work was supported by the National Natural Science Foundation of China (21573150, 21203122, 21566011, 31570560) and Jiangxi Province Sponsored Programs for Distinguished Young Scholars (20162BCB23026).

### References

- [1] L. Hintermann, A. Labonne, *Synthesis* 8 (2007) 1121–1150.
- [2] C.J. Li, B.M. Trost, *Proc. Natl. Acad. Sci.* 105 (2008) 13197–13202.
- [3] M. Nishizawa, H. Imagawa, H. Yamamoto, *Org. Biomol. Chem.* 8 (2009) 511–521.
- [4] F.X. Zhu, W. Wang, H.X. Li, *J. Am. Chem. Soc.* 133 (2011) 11632–11640.
- [5] Y. Xu, X. Hu, J. Shao, G. Yang, Y. Wu, Z. Zhang, *Green Chem.* 17 (2015) 532–537.
- [6] F. Trentin, A.M. Chapman, A. Scarso, P. Sgarbossa, R.A. Michelin, G. Strukul, D.F. Wass, *Adv. Synth. Catal.* 354 (2012) 1095–1104.
- [7] A. Mann, A. Wagner, *Chem. Commun.* 48 (2012) 434–436.
- [8] F. Chevallier, B. Breit, *Angew. Chem., Int. Ed.* 118 (2006) 1629–1632.
- [9] F. Boeck, T. Kribber, L. Xiao, L. Hintermann, *J. Am. Chem. Soc.* 133 (2011) 8138–8141.
- [10] W. Baidossi, M. Lahav, J. Blum, *J. Org. Chem.* 62 (1997) 669–672.
- [11] J.W. Hartman, W.C. Hiscox, P.W. Jennings, *J. Org. Chem.* 58 (1993) 7613–7614.
- [12] Z.W. Chen, D.N. Ye, Y.P. Qian, M. Ye, L. Liu, *Tetrahedron* 69 (2013) 6116–6120.
- [13] A. Mann, A. Wagner, *Chem. Commun.* 48 (2012) 434–436.
- [14] W. Liu, H. Wang, C.J. Li, *Org. Lett.* 18 (2016) 2184–2187.
- [15] T. Tsuchimoto, T. Joya, E. Shirakawa, Y. Kawakami, *Synlett* 12 (2000) 1777–1778.
- [16] A.S. Amarasekara, *Chem. Rev.* 116 (2016) 6133–6183.
- [17] J.P. Hallett, T. Welton, *Chem. Rev.* 111 (2011) 3508–3576.
- [18] V.I. Pârvulescu, C. Hardacre, *Chem. Rev.* 107 (2007) 2615–2665.
- [19] H. Xing, T. Wang, Z. Zhou, Y. Dai, *Ind. Eng. Chem. Res.* 44 (2005) 4147–4150.
- [20] F.J. Liu, L. Wang, Q. Sun, L. Zhu, X. Meng, F. Xiao, *J. Am. Chem. Soc.* 134 (2012) 16948–16950.
- [21] D.W. Kim, D.Y. Chi, *Angew. Chem., Int. Ed.* 43 (2004) 483–485.
- [22] V.I. Pârvulescu, C. Hardacre, *Chem. Rev.* 107 (2007) 2615–2665.
- [23] C. Sievers, O. Jimenez, T.E. Muller, S. Steuernagel, J.A. Lercher, *J. Am. Chem. Soc.* 128 (2006) 13990–13991.
- [24] M.-J. Jin, A. Taher, H.J. Kang, M. Choi, R. Ryoo, *Green Chem.* 11 (2009) 309–313.
- [25] F. Shi, Q. Zhang, D. Li, Y.-Q. Deng, *Chem.-Eur. J.* 11 (2005) 5279–5288.
- [26] F.J. Liu, X.-J. Meng, Y.-L. Zhang, L.-M. Ren, F. Nawaz, F.-S. Xiao, *J. Catal.* 271 (2010) 52–58.
- [27] A.M. Zheng, S.J. Huang, S.B. Liu, F. Deng, *Phys. Chem. Chem. Phys.* 13 (2011) 14889–14901.
- [28] W. Li, Z.J. Jiang, F.Y. Ma, F. Su, L. Chen, S.Q. Zhang, Y.H. Guo, *Green Chem.* 12 (2010) 2135–2138.
- [29] Q.H. Yang, J. Liu, J. Yang, M.P. Kapoor, S. Inagaki, C. Li, *J. Catal.* 228 (2004) 265–272.
- [30] Y. Chu, Z. Yu, A. Zheng, H. Fang, H. Zhang, S.J. Huang, S.B. Liu, F. Deng, *J. Phys. Chem. C* 115 (2011) 7660–7667.
- [31] A.M. Zheng, H. Zhang, X. Lu, S.B. Liu, F. Deng, *J. Phys. Chem. B* 112 (2008) 4496–4505.
- [32] N. Feng, A.M. Zheng, S.J. Huang, H. Zhang, N. Yu, C.Y. Yang, S.B. Liu, F. Deng, *J. Phys. Chem. C* 114 (2010) 15464–15472.
- [33] A.M. Zheng, S. Li, S.B. Liu, F. Deng, *Acc. Chem. Res.* 49 (2016) 655–663.
- [34] A.M. Zheng, S.B. Liu, F. Deng, *Chem. Rev.* 117 (2017) 12475–12531.
- [35] A.M. Zheng, S.J. Huang, W.H. Chen, P.H. Wu, H.L. Zhang, H.K. Lee, L.C. de Mênorval, F. Deng, S.B. Liu, *J. Phys. Chem. A* 112 (2008) 7349–7356.
- [36] V. Lucchini, G. Modena, *J. Am. Chem. Soc.* 112 (1990) 6291–6296.